Fermi National Accelerator Laboratory

FERMILAB-Conf-97/203-E
CDF

Kt-Jets and Jet Structure and Fragmentation at the Tevatron

Andrew Beretvas
For the CDF Collaboration

Fermi National Accelerator Laboratory
P.O. Box 500, Batavia, Illinois 60510

June 1997

Presented at the *5th International Workshop on Deep Inelastic Scattering and QCD (DIS 97)*, Chicago, Illinois, April 14-18, 1997

Operated by Universities Research Association Inc. under Contract No. DE-AC02-76CH03000 with the United States Department of Energy

Kt-Jets and Jet Structure and Fragmentation at the Tevatron

Andrew Beretvas*

* *Fermi National Accelerator Laboratory, Batavia Illinois 60510*

Abstract. $k_\perp$ algorithms are now used by both DØ and CDF to study jets. A preliminary study of jet structure for data taken by DØ and CDF during run I (92-95) is presented. DØ has measured the jet mass as a function of jet p_T. The CDF measurement of inclusive charged particle momentum distributions is in agreement with the Modified Leading Log Approximation (MLLA).

INTRODUCTION

In this paper, I report on four jet analyses done at the Tevatron. The data were taken by DØ and CDF in run I (1992-95). DØ has measured the average number of subjets as a function of the resolution variable (y_{cut}) [1]. For $y_{cut} = 0.01$, the radial subjet E_T flow is found as a function of ΔR around the jet axis. In the second analysis, CDF has found that the subjet radius for high E_T jets decreases as the subjet momentum increases. In the third analysis, jet mass is measured as a function of jet p_T for inclusive central jets [2]. This analysis was done by DØ using a $k_\perp$ algorithm. In the last analysis, the inclusive momentum distribution of charged particles in jets is measured using the CDF detector. $E_{Jet}\theta$ scaling is observed in agreement with the MLLA [3].

SUBJET STRUCTURE OF JETS AT DØ

DØ has used a $k_\perp$ algorithm to define jets [4]. Inclusive jets were reconstructed by preclustering calorimeter cells within a radius of 0.2 in $\eta - \phi$ space. In the $k_\perp$ algorithm, all 4-vectors in the event are merged together successively starting with the pair with the smallest relative p_T, stopping when no pair is within a distance D = 1.0 in $\eta - \phi$ space. The remaining 4-vectors are called jets. To resolve subjets within a jet, the algorithm is rerun on all 4-vectors within the jet. Merging stops when all 4-vectors pairs (i,j) have

$$d_{i,j} = \min(E^2_{T,i}, E^2_{T,j})(\Delta\eta^2_{i,j} + \Delta\phi^2_{i,j}) > y_{cut}E^2_{T,jet} \quad (1)$$

The resolution parameter y_{cut} defines the minimum relative transverse momentum between subjets inside the jet. In this analysis central jets are used ($|\eta| < 0.5$) with $275 < E_T^{jet} < 350$ GeV. Figure 1 shows that N_{sub} increases by $\approx 70\%$ as y_{cut} is decreased three orders of magnitude. The number of subjets is about 1.25 for $y_{cut} = 0.01$. Using this value of y_{cut}, DØ finds for jets with two subjets, it is most likely that one subjet near the jet axis carries most of the jet E_T near the jet axis, and the second subjet is much softer and further from the jet axis. For this same y_{cut} the radial distribution of subjet energy flow is in good agreement with HERWIG.

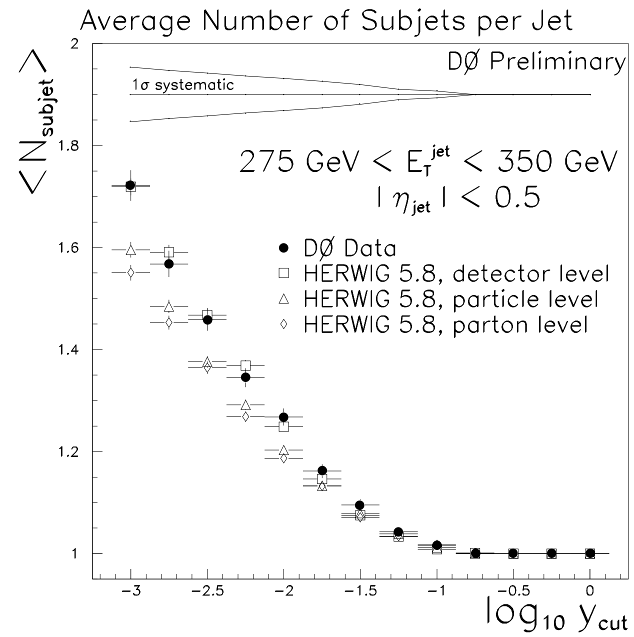

FIGURE 1. Average number of subjets per central high E_T jet vs. resolution variable y_{cut}. The error bar are statistical, and the $\pm 1\ \sigma$ systematic error band is an estimate of the effects of multiple interactions and energy scale correction error, added in quadrature.

SUBJETS AT CDF

Perturbative Quantum Chromodynamics predicts differential inclusive-jet and multi-jet cross sections by identifying hard final state partons with the energy flow in real events. A comparison of the internal properties of high-E_T jets with parton shower Monte Carlo predictions tests the physical ideas embodied in the evolution of the parton shower and the hadronization model. A set of high E_T (corrected $E_T > 140$ GeV) central jets ($0.1 < |\eta| < 0.5$) are selected for this analysis. The jets are found using a cone algorithm with radius 0.7 in $\eta - \phi$ space. The charged tracks are clustered into subjets using a $k_\perp$ algorithm. Fig. 2 shows the collimation of these high-E_T subjets as a function of the transverse momentum of the subjets. The width of subjets is defined as

$$r_{RMS} \equiv \frac{1}{n}\sqrt{\sum_{i=1}^{n}(\phi_i - \overline{\phi})^2 + (\eta_i - \overline{\eta})^2} \tag{2}$$

where n is the number of charged tracks in the subjet. The decrease in the subjet width as a function of subjet momentum is reproduced by HERWIG (5.6).

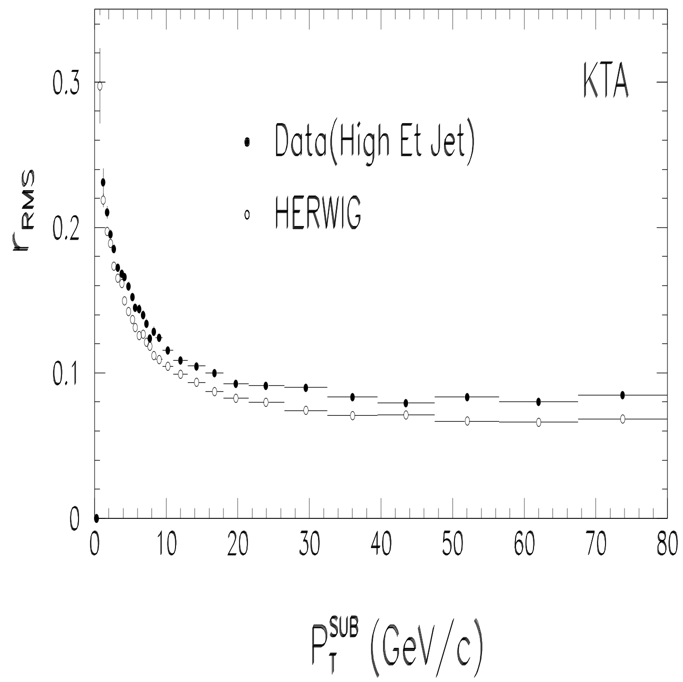

FIGURE 2. Subjet RMS radius versus subjet p_T^{SUB} (relative to the beam) for jets of E_T^{jet} > 140 GeV/c^2.

JET MASS MEASUREMENT AT DØ

The jet cone algorithm has known problems with jet overlap. The $k_\perp$ algorithm is more tractable theoretically. It is also possible that the $k_\perp$ algorithm will allow one to study physics which is not modeled in next-to-leading-order theory. Thus, the present analysis of jet mass as a function of jet p_T is done using a $k_\perp$ algorithm. Much effort has gone into correctly modeling showers and noise in the calorimeter.

The jet mass is defined in terms of the energy and momentum measured in the calorimeter

$$m = \sqrt{E^2 - p^2} \tag{3}$$

In the case of jets with $E_\perp$ evenly distributed in (η,ϕ) space with a two-dimensional Gaussian energy density distribution, one expects

$$m \sim \sqrt{2}\, p_T\, \sigma \tag{4}$$

where $\sigma = \sigma_\eta = \sigma_\phi$. The result, shown in Fig. 3, should not depend on which jet is used in a multijet event (The jets are selected to be free of trigger biases). A small difference was found between the leading jet (for p_T between 50 and 75 GeV/c) and the other jets in the event. The systematic error is dominated by the above effect, but is still small (less than 2%). The mass versus p_T is correctly predicted by HERWIG except at the lowest p_T's.

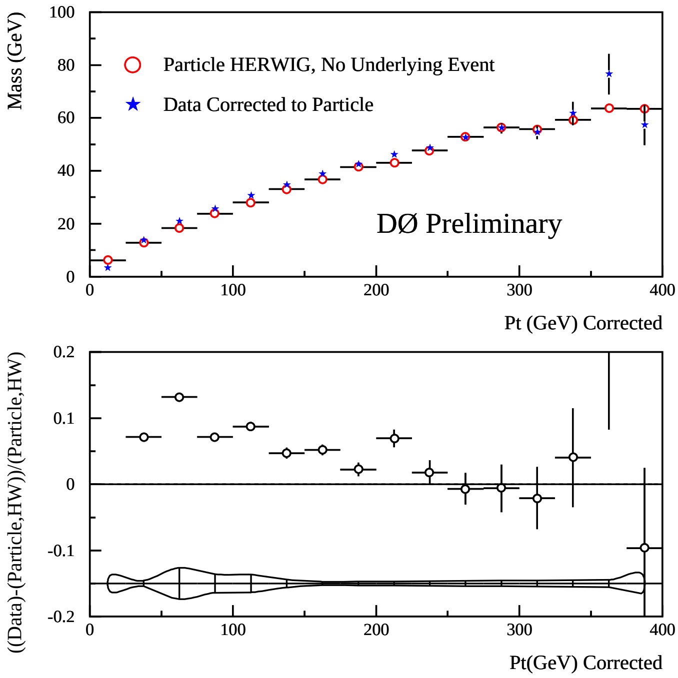

FIGURE 3. Jet mass as a function of p_T. The error bars are statistical. (a) Shows the mass vs. p_T curve for both data with all known corrections compared with HERWIG, without underlying event. (b) Shows the (data-theory)/theory. The bottom band denotes the systematic error.

INCLUSIVE CHARGED PARTICLE MOMENTUM DISTRIBUTIONS AT CDF

Inclusive charge particle momentum distributions have been measured at CDF. An analytic formula to describe these distributions has been derived in the framework of the Modified Leading Log Approximation. The important ideas are the angle ordering (partons can not be radiated at angles exceeding the angle of the proceeding emission) and that emission terms that contain both collinear and soft divergences can be summed. The data sample which consists of about 190,000 events is divided into 45 subsamples. These 45 subsamples contain 9 different dijet mass ranges from a low of $72 < M_{JJ} < 95$ GeV/c^2 to a high of $570 < M_{JJ} < 740$ GeV/c^2, and 5 different opening angles (θ_{cone} = 0.168, 0.217, 0.280, 0.361, and 0.466). A typical sample consists of events where the dijet mass is in the range $340 < M_{JJ} < 440$ GeV/c^2 and all tracks are contained within a cone of opening angle $\theta = 0.466$. The opening angles are relative to the jet axes. The data is fit with a analytic formula that contains two parameters Q_{eff} and const. Q_{eff} is the cutoff scale, and const is the number of hadrons to the number of final partons. For the typical curve ($\frac{1}{N_{events}}\frac{dN_{track}}{d\xi}$) versus $\xi = \ln(E_{jet}/p_{track})$ we obtain Q_{eff} = 234 ± 2 (stat) ± 20 (syst) MeV, const = 0.538 ± 0.002 (stat) $\pm\,^{0.080}_{0.040}$ (syst), with a χ^2/D.F. = 85.2/56 = 1.52.

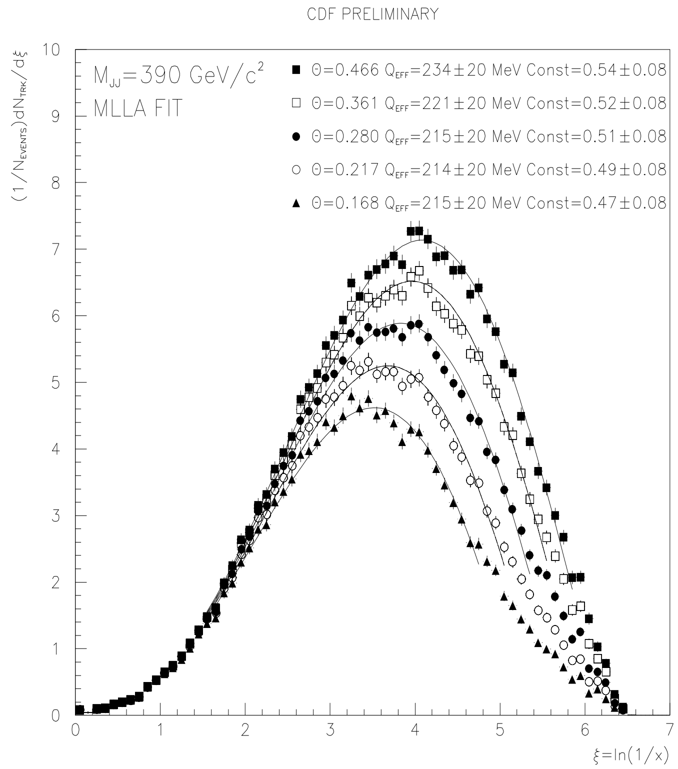

FIGURE 4. Evolution of inclusive momentum distributions with opening angle varying from 0.168 to 0.466. Fits are done according to the MLLA Limiting Spectrum.

Figure 4 shows the MLLA fits for five different opening angle cuts for a fixed dijet mass. Fits to the different subsets yield values almost identical to that of the typical sample. However, for a given dijet mass as the opening angle increases the peak of the curve shifts towards higher values of ξ. Figure 5 shows the peak position as a function of $M_{JJ}\ \Theta$. The data plotted show our data and points from TASSO, OPAL and ALEPH. Points from all 9 of the dijet mass ranges are plotted, showing scaling.

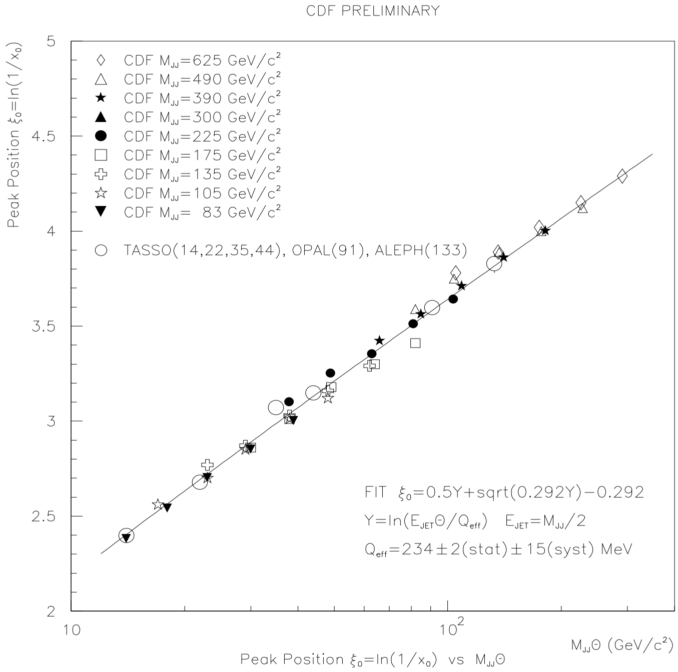

FIGURE 5. Evolution of the peak position vs. $M_{JJ}\Theta$. One can see that E_{Jet} scaling is observed. Fit is done according to the MLLA prediction.

ACKNOWLEDGMENTS

I would like to thank the organizers of this conference for their hospitality. Thanks also to my collaborators at CDF especially H. Akimoto, M. Binkley, S. Geer, A.T. Goshaw, A. Korytov and G.P. Yeh. D. Lincoln, H. Schellman and R. Snihur helped with the DØ parts of this paper. We would also like to thank Y. Dokshitzer for discussions. Finally, I would like to thank R. Herber for help with the PostScript.

REFERENCES

1. Snihur R., DPF Minneapolis Minn. (1996).
2. Lincoln D., Moriond Conference (1997), Fermilab-Conf-97/149-E.
3. Dokshitzer, YU.L., Khose, V.A., and Troyan, S.I., Int. J. Mod. Phys. **A7**, 1875 (1992).
4. Ellis, S.D. and Soper, D.E., Phys. Rev. D **48**, 3160 (1993).